Asymmetry of the magnetization reversal process in a magnetic tunnel junction

M. Cormier,[1,2,*] K. March,[1,2] J. Ferré,[1] A. Mougin,[1] and W. Raberg[3]
[1]*Laboratoire de Physique des Solides, Univ. Paris-Sud, CNRS, UMR 8502, F-91405 Orsay Cedex, France*
[2]*ALTIS Semiconductor, 224 boulevard John Kennedy, F-91105 Corbeil-Essonnes Cedex, France*
[3]*Infineon Technologies AG, Am Campeon 1-12, 85579 Neubiberg, Germany*
(Received 13 September 2007; revised manuscript received 19 December 2007; published 19 February 2008)

Field induced magnetization reversal dynamics of a soft magnetic layer embedded in a magnetic tunnel junction stack has been studied by magneto-optical magnetometry. Different dynamic behaviors are revealed comparing parallel-to-antiparallel and antiparallel-to-parallel reversals. Local inhomogeneities evidenced in the barrier thickness are transferred to the dipolar coupling field locally experienced by the soft layer, and are proposed as being at the origin of an asymmetry of nucleation and propagation processes accounting for the magnetization dynamics.

DOI: 10.1103/PhysRevB.77.054419 PACS number(s): 75.60.Jk, 75.70.Cn, 68.37.Lp

I. INTRODUCTION

Improvement in growth of magnetic and/or nonmagnetic artificial structures tailored on length scales characteristic of important interactions has led to the discovery of many physical properties. For example, in multilayers in which a ferromagnetic layer experiences a nonhomogeneous effective coupling field whose wavelength is larger than the exchange length, slight spatial fluctuations of the magnetic orientation are responsible for biquadratic or high order anisotropies.[1,2] This can result in various features on the ferromagnet, like shifted and/or complex hysteresis loops as well as nontrivial reversal mechanisms. The ferromagnet magnetization reversal can also depend on the orientation of the applied magnetic field with respect to the coupling field. This is frequent in exchange biased systems,[3–7] where this reversal asymmetry usually gives rise to an asymmetry of the macroscopic hysteresis loop shape. Only few results were reported so far on reversal asymmetry in a soft magnetic layer coupled to a harder one by dipolar interaction.[8,9] In this paper, we show that an asymmetry in the magnetization reversal can occur in spite of an apparently symmetric shape of the macroscopic hysteresis loop. Indeed, magnetic relaxation measurements are used to analyze the magnetization reversal of a magnetic tunnel junction's (MTJ) dipolar coupled soft layer. Magnetization reversal asymmetry is clearly evidenced: despite the hysteresis loop squareness, the measured reversal dynamics is different depending on the field sweeping direction. The tunnel barrier is investigated using transmission electron microscopy in order to evaluate its thickness variations and lateral wavelength modulations. We assert that the spatial fluctuation of the unidirectional dipolar coupling drives an asymmetry in domain nucleation and subsequent domain wall propagation fields, which accounts for our relaxation results.

II. EXPERIMENT

The [PtMn (17.50 nm)/CoFeB based pinning layer (1.90 nm)/Ru (0.85 nm)/CoFe reference layer (1.60 nm)/Al_2O_3/CoFeB soft layer (3.00 nm)] MTJ stack was grown by sputtering on a SiO substrate, with Ta based buffer and capping layers [Fig. 1(a)]. This stack was annealed in a magnetic field of 1 T in order to induce the antiferromagnetic phase of PtMn. This way the CoFe reference (R) layer is pinned and has a marked uniaxial planar magnetic anisotropy, which in turn fixes the easy axis of magnetization of the soft (S) CoFeB layer.

The S layer's magnetization is probed by Kerr magneto-optical magnetometry.[10] The longitudinal Kerr rotation (LKR), proportional to the sample magnetization over its illuminated area (about 0.03 mm^2), is measured at room temperature with green light (543.5 nm), under a magnetic field applied along the MTJ's anisotropy axis. This magnetic field is always weak enough to affect only the S layer, the R one staying saturated and pinned.

Conventional transmission electron microscopy (CTEM) was performed on a 200 kV TOPCON 002B instrument in bright field mode on a twin sample. The sample thickness was optimized, down to electron transparency, using tripod mechanical polishing on an area as large as possible (typically a few microns [Fig. 1(a)]).

III. RESULTS

A. Transmission electron microscopy

Bright field contrast CTEM images are shown in Figs. 1(a) and 1(b). On these images, the alumina layer appears thin and bright, whereas the other metallic layers look darker.

In order to get the thickness d of the alumina barrier and its lateral modulations, it is necessary to represent each interface (R/Al_2O_3 and Al_2O_3/S) by a single continuous line on the image.[11] The results obtained from the analysis of a 63 nm interface length (made of about 3000 pixels) are shown in Fig. 1(c). The measured d value is 1.55 ± 0.15 nm with a non-Gaussian distribution. The interfaces exhibit lateral modulations essential to understand the magnetic coupling between S and R layers: they are correlated on both sides of the tunnel barrier and have a roughness amplitude h estimated as 0.35 ± 0.05 nm with a dominant wavelength λ of 24 ± 3 nm.

B. Hysteresis loop

A typical minor hysteresis loop accounting for the S layer's macroscopic reversal is shown in Fig. 2. The

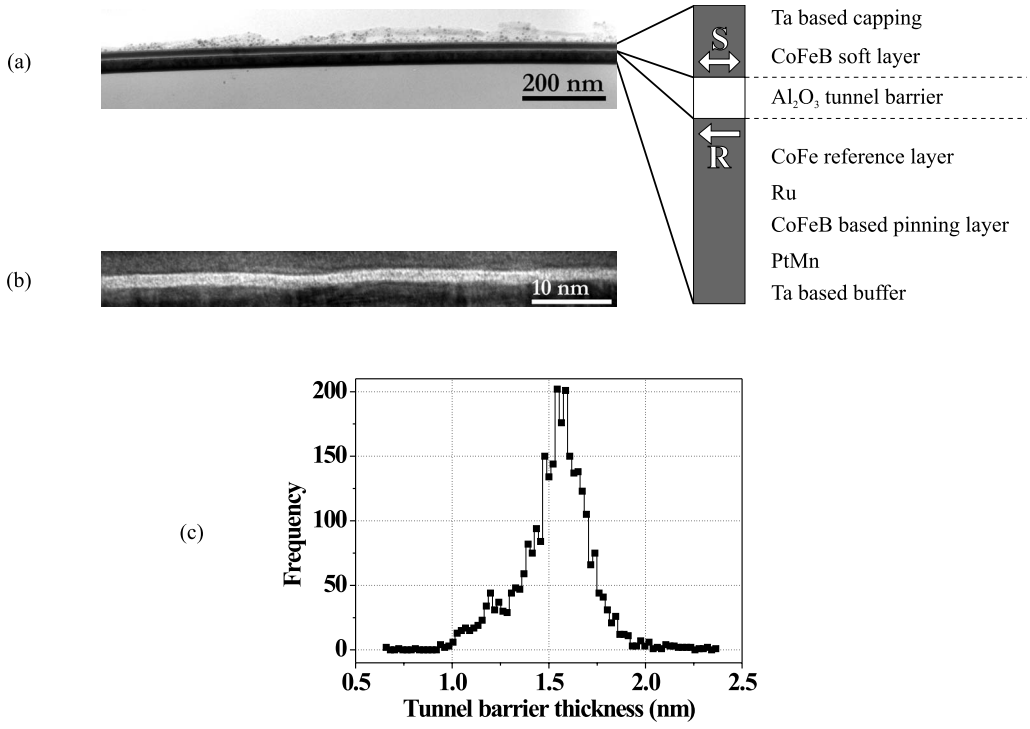

FIG. 1. Conventional transmission electron microscopy images, at (a) low and (b) high magnifications, of the MTJ stack. The alumina tunnel barrier thickness is measured as being $d=1.55\pm0.15$ nm. From image processing of (b), a non-Gaussian distribution of d is deduced (c). Frequency indicates the number of pixels among the 2944 x pixels of (b) yielding to the value of d.

5.9 ± 0.2 Oe loop shift with respect to zero field reveals the magnetic coupling between the S and R layers. The internal field, indeed, writes $H_{int}=H_{app}+H_{coupl}$: the applied field H_{app} has to balance a coupling field $H_{coupl}=-5.9\pm0.2$ Oe acting on S in order to trigger the S layer reversal. This coupling can be reasonably accounted for by the Néel dipolar orange-peel coupling:[12–15]

$$H_{coupl}=-\frac{\pi^2}{\sqrt{2}\lambda}\frac{h^2}{t_S}M_s^R e^{-2\pi\sqrt{2}d/\lambda}, \quad (1)$$

where t_S is the S layer thickness (3 nm) and M_s^R the saturation magnetization of the reference layer ($M_s^R=1250$ erg G^{-1} cm^{-3}).[16] Making use of transmission electron microscopy investigations giving values for d, h, and λ, we get a coupling field of -8 ± 4 Oe, consistent with the measured value. The orange-peel coupling field is, thus, certainly the predominant coupling contribution in our system; it is ferromagnetic, as predicted for correlated interface roughnesses on both sides of the tunnel barrier, and, thus, favors a parallel (P) magnetization alignment in the S and R layers with respect to an antiparallel (AP) one. Unlike coercive fields values, H_{coupl} is found to be constant when increasing the magnetic field sweep rate (at least from 14 Oe s^{-1} to 2.9 kOe s^{-1}). This is consistent with previous data obtained in a NiFe/Cu/Co spin-valve stack,[17] in which the NiFe layer is submitted to a similar dipolar orange-peel coupling.

C. Magnetic relaxation

The inset of Fig. 2 summarizes the principle of magnetic relaxation measurements,[10] performed at room temperature on both branches of the minor hysteresis loop. The S layer is first saturated in the AP (P) configuration by applying a $H_{sat}^{AP(P)}=+(-)18$ Oe field. Then, at time $t=0$, the applied field is quickly set to a value $H_{app}^{AP\text{-}P(P\text{-}AP)}$, close to the coercive field H_{c1} (H_{c2}). The applied field is then kept constant, and the sample's magnetization is measured by LKR as a function of time t.

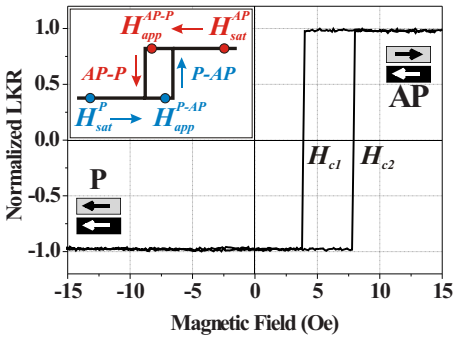

FIG. 2. (Color online) Minor hysteresis loop of the MTJ sample, measured by LKR with a magnetic field sweep rate of 14 Oe s^{-1}. The relative orientations of the two S and R layers' magnetizations are reported on the graph. The coercive fields of S are $H_{c1}=+3.9\pm0.2$ Oe for the decreasing (AP-P) branch of the loop, and $H_{c2}=+7.9\pm0.2$ Oe for the increasing (P-AP) branch. Inset: Principle of magnetic relaxation experiments, as detailed in the text.

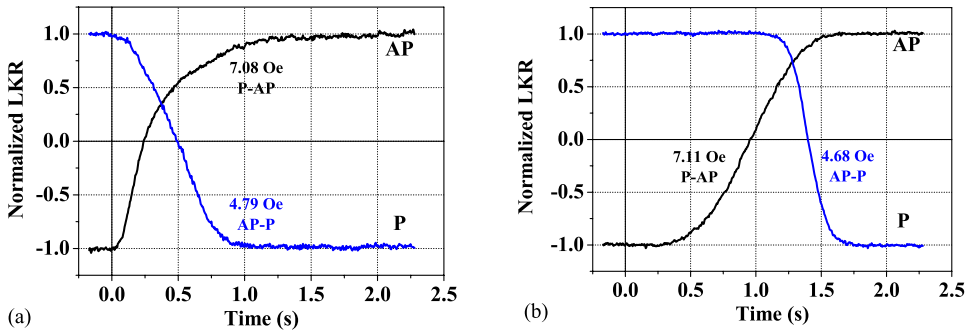

FIG. 3. (Color online) LKR magnetic relaxation curves of the MTJ's soft layer, for two different probed regions (a) I and (b) II of the sample, separated by about 3 mm. Values of the corresponding $H_{app}^{AP\text{-}P(P\text{-}AP)}$ fields are reported on the curves. On each graph, the two curves, associated with the two (AP-P and P-AP) reversal types, correspond to quasi-identical internal magnetic fields in the probed layer. Each curve is an average over five similar reversals. After each reversal, the system is resaturated by applying a field $H_{sat}^{AP(P)}=+(-)18$ Oe.

Relaxation curves, obtained in two different regions I and II of the sample, are shown in Fig. 3. In each region, the AP-P and the P-AP reversals correspond to equivalent values of the internal magnetic field, that is, to equivalent distances from the AP-P and P-AP coercive fields values, H_{c1} and H_{c2}.[18] These data show that the relaxation behavior depends both on the probed region and on the reversal direction. In region I [Fig. 3(a)], both reversals start nearly immediately once the field step is applied to the sample. However, for the P-AP case, the relaxation curve has a quasiexponential shape, whereas for the AP-P reversal, the magnetization begins to decrease quadratically. Besides, in region II [Fig. 3(b)], the relaxation curves both show a delay between the field step and the beginning of the reversal, and both have a symmetrical S shape. Nevertheless, the delay is roughly four times greater, and the reversal duration shorter, for the AP-P reversal than for the P-AP one.

IV. DISCUSSION

A. Reversal modes

Magnetization reversal in a magnetic material involves the nucleation of domains followed by domain wall propagation or coherent rotation of the magnetization.[10] If we assume that one single domain wall propagates through the probed area, the domain wall velocity is in the 10^{-4} m s^{-1} range. This is a very low value since domain wall velocities of several tens of m s^{-1} can be reached,[10] and, therefore, rules out a — faster — reversal by coherent rotation of the magnetization. Thermally activated domain nucleation and wall propagation[19,20] are, thus, responsible for the observed types of reversal. The corresponding nucleation rate n and mean wall velocity v, which determine the reversal dynamics, are proportional to the switching probability of elementary activation volumes V_{act}^{n} and V_{act}^{v}, respectively,[19,20] which, of course, depend on the film's internal structure.[10,21] Let us consider, for instance, the nucleation rate n:

$$n = n_0 \exp\left[\frac{2M_s V_{act}^{n}}{k_B T}(H_{int} - H_{nucl})\right], \qquad (2)$$

where k_B is the Boltzmann constant, T the temperature, and M_s the saturation magnetization (for our CoFeB S layer,[16] $M_s=800$ erg G^{-1} cm^{-3}). H_{int} is the internal applied magnetic field (here, $H_{int}=H_{app}^{P\text{-}AP(AP\text{-}P)}+H_{coupl}$). H_{nucl} is the nucleation field setting the upper boundary of the thermally activated regime. It is usually slightly higher than the coercive field, the difference between them depending only on the reversal dynamics.[10] $(H_{int}-H_{nucl})$ denotes the difference between the applied field and the nucleation field, and, thus, indirectly reflects the difference between the applied field and the coercive field. n_0 is the limit nucleation rate reached for $H_{int}=H_{nucl}$. Applying Eq. (2) to relaxation curves obtained with different applied field values, we deduce a reasonable estimation of $V_{act}^{n}\approx 10^5$ nm^3 in our sample.[22] This leads to a characteristic lateral size of a few hundreds of nanometers for the initially nucleated reversed center. H_{nucl} is also estimated to a few oersteds. A relation similar to Eq. (2) holds for the wall velocity v with the propagation field,[19] H_{prop}. One may notice that in these relaxation experiments (Fig. 3), the resulting reversal occurs for a lower applied field as compared to that expected from the minor hysteresis loop (Fig. 2). Usually, the higher the sweep rate of the applied field, the larger the coercivity.[10] In relaxation experiments, the system is kept under a constant field value until the reversal occurs. The field sweep rate, thus, tends to zero, and the reversal field is reduced as compared to the coercive field measured on the minor hysteresis loop.

Three characteristic domain wall mediated mechanisms (Fig. 4) can be envisioned for the magnetization reversal in the illuminated area of our sample: (a) nucleation dominated process, characterized by a quasiexponential relaxation;[10,19,23] (b) pure domain wall propagation in the probed area due to the expansion of rare outside nucleated domains, which implies S-shape-type relaxation curves, as may be checked by considering a plane wall crossing a circular probed area; and (c) domain nucleation within the probed area and prevailing subsequent domain expansion. The relaxation curve shape is then slightly more complex: it is quadratic in time as long as reversed domains are entirely contained in the probed area, and gradually slows when the walls get out of this area.[10]

The quasiexponential shape of the P-AP relaxation curve for region I [Fig. 3(a)] is, thus, likely to result from many nucleation events within the probed area [Fig. 4(a)], whereas the quadratic beginning of the AP-P relaxation curve in the

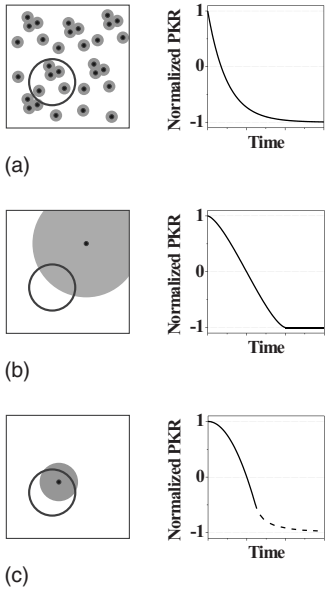

FIG. 4. Sketch of domain wall mediated magnetization reversal processes in the probed area (sketched by a black circle in each case) of our sample (left) and of the typical shapes of the associated relaxation curves (right): (a) nucleation dominated reversal, giving rise to a quasiexponential relaxation curve; (b) pure domain wall propagation due to the expansion of an outside nucleated domain, giving rise to an S-shape-type relaxation curve; and (c) nucleation of a domain within the probed area and subsequent expansion, giving rise to a quadratic beginning of the relaxation curve. Black dots and gray disks stand for nucleation centers and reversed domains, respectively.

same region rather results from one or a few nucleation events within the probed area and a prevailing subsequent domain expansion [Fig. 4(c)]. The instantaneous reaction of the reversal to the applied field in both cases implies a short nucleation time. Besides, the quasi-S-shape of both relaxation curves in region II [Fig. 3(b)] is likely to result from the propagation of one or a few domain walls through the probed area, coming from nucleation centers located outside this area [Fig. 4(b)]. This kind of reversal can only be detected when the wall goes across the spot, i.e., after a lag time, which includes a probabilistic nucleation delay, and a propagation time which depends on the location of the nucleation center. Namely, the longer delay observed before the beginning of the AP-P transition in region II is indicative of a nucleation center which is less reactive and/or located at a greater distance from the spot, as compared to the one involved in the P-AP reversal.

This leads us to three main conclusions: (i) there is a spatial inhomogeneity of nucleation centers in S, probably due to tiny, large scale topological fluctuations of the tunnel barrier thickness, leading to more nucleation centers in region I than in region II; (ii) in region I [Fig. 3(a)], there are more nucleation centers for the P-AP reversal than for the AP-P one; and (iii) in region II [Fig. 3(b)], nucleation originates from different centers for the two reversal directions, and domain wall propagation is faster for the AP-P reversal than for the P-AP one.

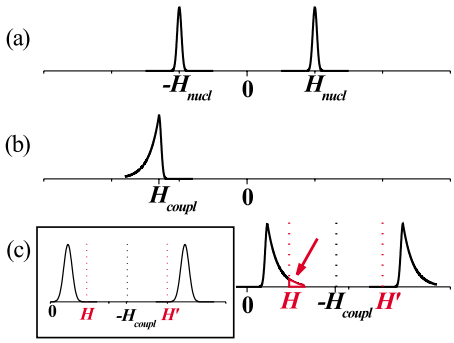

FIG. 5. (Color online) Sketch of (a) nucleation field distribution in an uncoupled layer, (b) asymmetrical distribution of the local coupling field in a dipolar coupled system, and (c) effective nucleation field distributions in the magnetic layer described in (a) combined with the local coupling field distribution shown in (b). H and H' stand for applied field values symmetrical with respect to $-H_{coupl}$: the nucleation centers activated for H and H' are not the same (see arrow). The effective nucleation field distribution corresponding to the case of a symmetrical coupling field distribution is sketched in the inset. The shape of the distributions is deliberately exaggerated. Their amplitudes are arbitrary.

B. Asymmetry between antiparallel-to-parallel and parallel-to-antiparallel reversals

We now focus on the observed asymmetry between the P-AP and AP-P reversal processes.

Domain nucleation and wall propagation in uncoupled and weakly defected layers are known as symmetrical processes with respect to the applied field: the associated H_{nucl} and H_{prop} fields are the same for negative or positive applied fields. H_{nucl} and H_{prop} are, in fact, local quantities, and one must consider nucleation [as sketched in Fig. 5(a)] and propagation field distributions.[24] If one considers a dipolar coupled layer such as S in our sample, the effective nucleation field at a given point of the layer is shifted by the local coupling field H_{coupl}^{local} with respect to that of the uncoupled layer. If the H_{coupl}^{local} distribution is symmetrical, the effective nucleation field distribution is also symmetrical, as sketched in the inset of Fig. 5: two applied magnetic fields H and H', symmetrical with respect to the macroscopic average $-H_{coupl}$, result in symmetrical nucleation processes. In our S layer, the local coupling field decreases when the tunnel barrier thickness d increases,[14,15] according to $e^{-d/\lambda}$ [Eq. (1)]. This implies that for the local coupling field, a slight decrease in d with respect to its macroscopic value produces a much higher difference than the equivalent increase in d. Even in the case of a barrier that would exhibit a random distribution of thickness d over the sample, the coupling field would be expected to be asymmetric since, by definition, the exponential of a Gaussian random variable is a lognormal random variable.[25] In our case, starting already from a nonsymmetric d distribution [Fig. 1(c)], we all the more expect an asymmetrical local coupling field distribution as sketched in Fig. 5(b). The enlarged extension toward the high local coupling field values corresponds to the low d values, that is, to the thinnest parts of the sample. Asserting such a local coupling field distribution, the effective nucleation field dis-

tribution has the shape sketched in Fig. 5(c). The applied magnetic fields H and H', symmetrical with respect to the macroscopic average $-H_{coupl}$, then obviously result in asymmetric nucleation processes. Indeed, for a low-field reversal, the amount of activated nucleation sites is greater and more spread than for the high-field reversal. In counterpart, the nucleation process triggers more sharply for the high-field reversal than for the low-field one.

Going back to our MTJ stack, this means that for the AP-P reversal (Fig. 2), nucleation appears more gradually but at a lower internal field than for the P-AP reversal. Actually, for the AP-P reversal, the first nucleation sites to be activated are those where the tunnel barrier is the thinnest (where coupling is the strongest), whereas for the P-AP reversal, the thickest parts of the sample (where coupling is the weakest) are activated first. This shows that the active nucleation centers in a coupled system are not the same for the two reversal types,[8] which is consistent with our experimental data. The same statement (and Fig. 5 as well) can apply to the propagation field distribution which characterizes wall motion, leading to a propagation at a lower internal field for the AP-P reversal as compared to the P-AP one.

Given the processes which were experimentally evidenced in the two regions of our sample, nucleation and propagation can be separately discussed. In region I [Fig. 3(a)], the only process that can be quantitatively compared between the AP-P and P-AP reversals is nucleation. The observed more efficient nucleation process during the P-AP reversal in this region is consistent with an expected sharper triggering of nucleation for this reversal type. Besides, in region II [Fig. 3(b)], only propagation can be quantitatively compared between the AP-P and P-AP reversals. The observed easier propagation during the AP-P reversal in this region is consistent with propagation at a lower internal field for the AP-P reversal as compared to the P-AP one, which was discussed above.

V. SUMMARY

Magnetization relaxation experiments have been performed on the soft electrode of a MTJ sample. In spite of a perfectly square hysteresis loop, they clearly show a reversal dynamics asymmetry between the AP-P and the P-AP reversals. In both cases, the reversal occurs by domain nucleation and wall propagation. To account for the observed differences in the soft layer, depending on the field sweeping direction relative to the macroscopic dipolar coupling field between the soft and reference layers, an asymmetry of nucleation and propagation processes is proposed. Through an inhomogeneous barrier, the dipolar coupling is turned into a lognormal-like distribution of effective fields, which accounts for the existence of locally preferential nucleation sites as well as for the differences in dynamics between the AP-P and the P-AP reversals. Finally, magnetic relaxation is shown to be a simple tool for deducing tiny changes in dynamics and for identifying processes usually evidenced by magnetoimaging techniques.

ACKNOWLEDGMENTS

This research was performed in the frame of a collaboration between the Université Paris-Sud and ALTIS Semiconductor. M.C. and K.M. thank the latter and the French ANRT for CIFRE financial support.

*cormier@lps.u-psud.fr

[1] B. Dieny and A. Vedyayev, Europhys. Lett. **25**, 723 (1994).
[2] J. C. Slonczewski, Phys. Rev. Lett. **67**, 3172 (1991).
[3] V. I. Nikitenko, V. S. Gornakov, A. J. Shapiro, R. D. Shull, K. Liu, S. M. Zhou, and C. L. Chien, Phys. Rev. Lett. **84**, 765 (2000).
[4] B. Beckmann, U. Nowak, and K. D. Usadel, Phys. Rev. Lett. **91**, 187201 (2003).
[5] J. McCord, R. Schäfer, R. Mattheis, and K.-U. Barholz, J. Appl. Phys. **93**, 5491 (2003).
[6] F. Romanens, S. Pizzini, F. Yokaichiya, M. Bonfim, Y. Pennec, J. Camarero, J. Vogel, J. Sort, F. Garcia, B. Rodmaq, and B. Dieny, Phys. Rev. B **72**, 134410 (2005).
[7] J. Camarero, J. Sort, A. Hoffmann, J. M. García-Martín, B. Dieny, R. Miranda, and J. Nogués, Phys. Rev. Lett. **95**, 057204 (2005).
[8] X. Portier, A. K. Petford-Long, R. C. Doole, T. C. Anthony, and J. A. Brug, Appl. Phys. Lett. **71**, 2032 (1997).
[9] K. Fukumoto, W. Kuch, J. Vogel, J. Camarero, S. Pizzini, F. Offi, Y. Pennec, M. Bonfim, A. Fontaine, and J. Kirschner, J. Magn. Magn. Mater. **293**, 863 (2005).
[10] J. Ferré, in *Spin Dynamics in Confined Magnetic Structures I*, edited by B. Hillebrands and K. Ounadjela, in Topics in Applied Physics Vol. 83 (Springer-Verlag, Berlin, Heidelberg, 2002), pp. 127–165.
[11] This process may be complicated by contrast variations on both R and S layers. The first step of image processing is to remove these variations thanks to thresholding. Then, Sobel filter is used to detect the position of each interface.
[12] L. Néel, C. R. Hebd. Seances Acad. Sci. **255**, 1676 (1962).
[13] J. Moritz, F. Garcia, J. C. Toussaint, B. Dieny, and J. P. Nozières, Europhys. Lett. **65**, 123 (2004).
[14] P. Fuchs, U. Ramsperger, A. Vaterlaus, and M. Landolt, Phys. Rev. B **55**, 12546 (1997).
[15] H. D. Chopra, D. X. Yang, P. J. Chen, D. C. Parks, and W. F. Egelhoff, Phys. Rev. B **61**, 9642 (2000).
[16] T. Dimopoulos, G. Gieres, J. Wecker, N. Wiese, and M. D. Sacher, J. Appl. Phys. **96**, 6382 (2004).
[17] Y. Pennec, J. Camarero, J. C. Toussaint, S. Pizzini, M. Bonfim, F. Petroff, W. Kuch, F. Offi, K. Fukumoto, F. Nguyen Van Dau, and J. Vogel, Phys. Rev. B **69**, 180402(R) (2004).
[18] The relaxation curves shown in the graphs are typical of the probed region of the sample and of the reversal type. In one single region of the sample (I or II), the AP-P and the P-AP reversals were obtained in the very same experimental conditions, so they can be compared quantitatively. However, the reversals observed in region I of the sample should be compared only qualitatively to those observed in region II.

[19] M. Labrune, S. Andrieu, F. Rio, and P. Bernstein, J. Magn. Magn. Mater. **80**, 211 (1989).
[20] A. Kirilyuk, J. Ferré, V. Grolier, J.-P. Jamet, and D. Renard, J. Magn. Magn. Mater. **171**, 45 (1997).
[21] S.-B. Choe, Y.-C. Cho, H.-J. Jang, and S.-C. Shin, J. Magn. Magn. Mater. **240**, 308 (2002).
[22] S. Boukari, R. Allenspach, and A. Bischof, Phys. Rev. B **63**, 180402(R) (2001).
[23] E. Fatuzzo, Phys. Rev. **127**, 1999 (1962).
[24] J. Ferré, V. Grolier, P. Meyer, S. Lemerle, A. Maziewski, E. Stefanowicz, S. V. Tarasenko, V. V. Tarasenko, M. Kisielewski, and D. Renard, Phys. Rev. B **55**, 15092 (1997).
[25] V. Da Costa, M. Romeo, and F. Bardou, J. Magn. Magn. Mater. **258**, 90 (2003).